

THE STUDY OF RELATIONSHIP BETWEEN THE GROUND TARGETS
SPECTRAL DATA AND ATM DATA

Zhang Z.G.
Centre For Remote Sensing In Geology
29 College Road, Beijing 100083, P.R.C.
Commission 7

Abstract : In this paper, based on analysing action between magnetoelectric wave through the atmosphere and the ground targets each other, mathematical model of the relationship between the ground targets spectral data and ATM data is derived from theory, and the physical significance of correlation parameters are given . According to ATM data(DS-1268 Scanner) and the spectral data of the field synchronization measurements (IRIS Spectroradiometer) at three test fields(Goldsea lake, Gaoyang and Anxin county), by using the analysis method of the statistical regression, the linear regression equations between the DN of each band of ATM(total twelve bands) and the reflectance brightness of the ground correspondence wavelength are obtained under all kinds of conditions, (such as different test fields, periods, flight heights and detection angles etc.). Taking advantage of this quantitative relationship equation, the original images of ATM are directly transformed into the ground efficient reflectance brightness images. In the transformation procedure, the atmospheric transmittance and path's radiance don't need to know. The efficient reflectance brightness images is able to reflect the ground targets spectral properties. Therefore, the effects of the atmosphere between the ground and the DS-1268 sensor are eliminated, and the image order is apparently improved. Moreover, the relationships between the atmospheric transmissivity and flight heights, detection angles and the atmospheric transmissivity are discussed.

KEY WORDS: Theory, Spectral, Image Processing, Multispectral.

1. INTRODUCTION

We know, the multispectral data of the space and aeronautics remote sensing are the reflective and radiant results of the earth objects. Aeronautic remote sensing data has not only to do with reflective properties of the earth objects, but also with the sun illuminance, atmospheric transmittance properties and sensitive properties of sensor. This paper tries to quantitatively study the relationship between the ATM data and spectral data of the earth objects. Although this is a very important work, it is doubtless on the deeping remote sensing technique and data quantitative application of remote sensing, the research is very difficult and complex.

2. THEORETICAL MODEL

The electromagnetic wave reflected and radiated by earth objects is measured, it is foundation of remote sensing technique. So as to quantitative approach relationship between airborne multispectral data and reflective properties of earth objects, it is very necessary that relation model of sensor response and reflective property of earth objects is created, this model is named for remote sensing equation in the paper[4]. Regardless space or aeronautic remote sensing technique, when their sensors measure earth objects, the electromagnetic waves all go through the atmosphere. Generally, the atmospheric effects are considered in the remote sensing equation, it is expressed as:

i. Because of the atmospheric absorption and diffusion, the sun radiation from atmospheric outer does not all reach the ground; there is a part of radiation from earth objects reflecting can enter the sensor.

ii. Because of the atmospheric diffusion, radiation without reaching the earth has small part radiation entering the sensor.

iii. The reflective radiance of around the object, because of the atmospheric diffusion, a part of that

enters the sensor.

If one assume: B is total radiant brightness. Ba is atmospheric radiance brightness of direct entering sensor. Bb is the radiance brightness of background. Bt is the targets reflective radiance brightness. Then, one obtains equation:

$$B = B_a + B_b + B_t \quad (1)$$

now, the other conditions are considered:

- i. Wavelength ranges is from λ_1 to λ_2 .
- ii. The solar zenith is θ .
- iii. The surface of earth objects is approximation to Lambertian surface.
- iv. The sun's irradiance distribution in the outer atmosphere is $E_o(\lambda)$.

Then, I. The atmospheric radiant brightness (shown in Fig.1) is expressed as:

$$B_a = \int_{\lambda_1}^{\lambda_2} \frac{1}{\pi} E_o(\lambda) \beta(\lambda) d\lambda \quad (2)$$

Where $\beta(\lambda)$ is the atmospheric efficient brightness. It depends on the atmospheric properties.

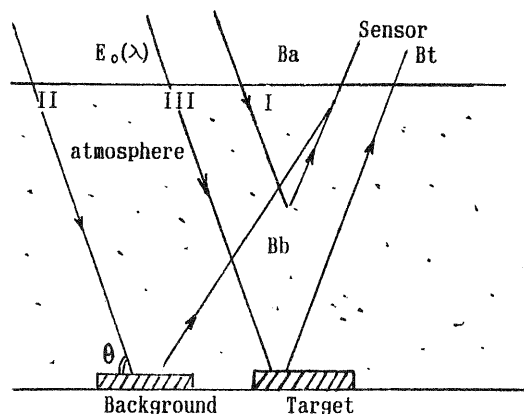


Fig.1 The relation of incident radiance atmosphere, background, target, reflective radiance and sensor. II. The radiant brightness of background reflection (Bb) is expressed as:

$$B_b = \int_{\lambda_1}^{\lambda_2} \frac{1}{\pi} E_0(\lambda) \sin\theta \tau_0(\lambda) \bar{\rho}(\lambda) \tau_s(\lambda) d\lambda \quad (3)$$

where $\bar{\rho}(\lambda)$ is the average reflectance of background. $\tau_0(\lambda)$ is atmospheric transmittance (direction of incident). It depends on the atmospheric diffusion properties. $\tau_s(\lambda)$ is the atmospheric transmittance of reflective direction.

III. The radiant brightness (Bt) is from the reflection of the target cross atmosphere it has not only to do with the target reflectance, but also with atmospheric absorption, diffusion properties and transmission path. It is expressed as:

$$B_t = \int_{\lambda_1}^{\lambda_2} \frac{1}{\pi} E_0(\lambda) \sin\theta \tau_0(\lambda) \rho(\lambda) \tau_z(\lambda) d\lambda \quad (4)$$

where $\rho(\lambda)$ is the reflectance of target. $\tau_z(\lambda)$ is direct transmittance. It's only depended on atmospheric absorption and diffusion in the reflective direction.

If the $S(\lambda)$ is the spectral response function of the sensor, then the total response(D) of the sensor is expressed as:

$$D = \int_{\lambda_1}^{\lambda_2} \frac{1}{\pi} E_0(\lambda) S(\lambda) [\beta(\lambda) + \tau_0(\lambda) \sin\theta (\bar{\rho}(\lambda) \tau_s(\lambda) + \rho(\lambda) \tau_z(\lambda))] d\lambda \quad (5)$$

when earth objects are very even within large area, $\bar{\rho}(\lambda)$ of the background is about $\rho(\lambda)$ of targets. One let:

$$\tau(\lambda) = \tau_s(\lambda) + \tau_z(\lambda) \quad (6)$$

where $\tau(\lambda)$ is the total transmittance of the atmosphere in direction of incident and reflective radiance. Thus the equation(5) is changed into the equation:

$$D = \frac{1}{\pi} \int_{\lambda_1}^{\lambda_2} E_0(\lambda) S(\lambda) [\beta(\lambda) + \sin\theta \tau_0(\lambda) \tau(\lambda) \rho(\lambda)] d\lambda \quad (7)$$

As to the remote sensing system of airborne multi-spectral scanner, let i indicate band, j indicate earth objects. Then equation(7) is rewritten as:

$$D_{ij} = \frac{1}{\pi} \int_{\lambda_{i1}}^{\lambda_{i2}} E_0(\lambda) S_i(\lambda) [\beta(\lambda) + \sin\theta \tau_0(\lambda) \tau(\lambda) \rho_j(\lambda)] d\lambda \quad (8)$$

Because Daedalus enterprise Incorporation. That Supplied us with relative response functions $S_{ri}(\lambda)$. Make

$$S_i(\lambda) = S_{pi}(\lambda) * S_{ri}(\lambda) \quad (9)$$

where $S_{pi}(\lambda)$ is the peak of response functions $S_i(\lambda)$.

$$E_e(\lambda) = E_0(\lambda) \sin\theta \tau_0(\lambda) \quad (10)$$

where $E_e(\lambda)$ is a irradiance distribution of the sun on the earth.

Considering designed band in the window of the atmosphere, the band is comparative narrow, in this case, $\tau(\lambda)$ is taken the place with τ_i . Then,

$$D_{ij} = \frac{1}{\pi} \int_{\lambda_{i1}}^{\lambda_{i2}} E_0(\lambda) S_{pi}(\lambda) S_{ri}(\lambda) \beta(\lambda) d\lambda + \frac{1}{\pi} \int_{\lambda_{i1}}^{\lambda_{i2}} E_e(\lambda) S_{pi}(\lambda) S_{ri}(\lambda) \tau_i \rho_j(\lambda) d\lambda \quad (11)$$

that is

$$D_{ij} = S_{pi} (L_{i0} + \tau_i L_{ij}) \quad (12)$$

in this equation,

$$L_{i0} = \frac{1}{\pi} \int_{\lambda_{i1}}^{\lambda_{i2}} E_0(\lambda) S_{ri}(\lambda) \beta(\lambda) d\lambda \quad (13)$$

$$L_{ij} = \frac{1}{\pi} \int_{\lambda_{i1}}^{\lambda_{i2}} E_e(\lambda) S_{ri}(\lambda) \rho_j(\lambda) d\lambda \quad (14)$$

where L_{i0} is the efficient reflective brightness of atmospheric diffusion associated the band and sensor response. It isn't associated with the earth objects. L_{ij} is the efficient reflective brightness of targets associated with the band response of the sensor.

If even considering DS-1268 with different gain channels of selection, so as to acquire reasonable read number under the different irradiance condition, without radiant energy entering the sensor, there is still read number output. It is called as zero input response(L_{oi}). Thus equation(12) is supposed to

$$D_{ij} = g_i S_{pi} (L_{i0} + \tau_i L_{ij}) + L_{oi} \quad (15)$$

equation(15) is reversed into the efficient reflective brightness of the earth objects. That is

$$L_{ij} = - \left(\frac{L_{i0}}{\tau_i} + \frac{L_{oi} g_i}{g_i S_{pi} \tau_i} \right) + \frac{D_{ij}}{g_i S_{pi} \tau_i} \quad (16)$$

or

$$L_{ij} = a_i + b_i * D_{ij} \quad (17)$$

where a and b are expressed as

$$a_i = - \left(\frac{L_{i0}}{\tau_i} + \frac{L_{oi} g_i}{g_i S_{pi} \tau_i} \right) \quad (18)$$

$$b_i = 1 / g_i S_{pi} \tau_i \quad (19)$$

where a is efficient radiance brightness of atmospheric diffusion and response of the sensor, b is the efficient reflective brightness variation of the earth objects. As above the equation(17) shows that relationship between the efficient reflective brightness of the earth objects (L_{ij}) and total response(D) with sensor each band is linear relation. This is the theory model of the paper.

3. TEST ARRANGEMENT AND DATA ACQUISITION

3.1 Be Ready Before Test

i. The reflectances of selected the earth objects are steady in the short time (e.g., highway, water, soil, living vegetation, and the man-made cloth targets ect.).

ii. There is some number about the type of earth objects. So as to make the regression equation be reliable, one considers the requirement of each band and the practical situation, selects seven to ten types of earth objects, also selects the different color cloth targets (size is 6 x 6 m²), they are snow white, yellow white, light grey, dark grey and black color clothes targets. Being ready cloth targets is for Winter, in which there are only a few natural earth objects.

iii. The reflectance values of selected earth objects have such a extent that it includes all kinds of possible reflective properties with each band. The reflectance from 0 to 100 percent is distributed to the full extent equably in all kinds of types earth objects.

iv. The sizes of the earth objects are enough large for the pixel area, and the reflective properties are steady. If pixel's area is $2.5 \times 2.5 \text{ M}^2$, in order to acquire a pure pixel (no mixture-pixel), the size of cloth targets is $5 \times 5 \text{ M}^2$ at least.

v. Select earth objects which have fairly good Lambert property. To avoid the influence of incident and view angle, one measures the Lambert property of cloth target before test. In addition, avoid taking place the primary and recall reflection being measured the water.

vi. Select the level earth objects for convenience.

3.2 Be Ready The Instruments

The calibration of IRIS Spectroradiometer. In order to obtain the correction reflectance data, IRIS Spectrometer must be calibrated again, and the gain/dark current file, detector function file, wavelength file are recreated, the radiance calibration was done, the new radiance file was created. Thus, the sun spectral irradiance is measured with IRIS Spectrometer (Fig.2).

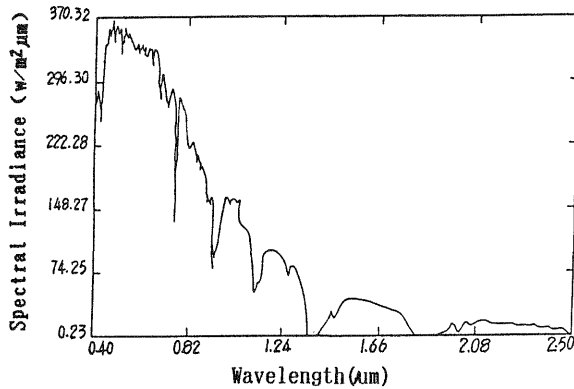


Fig.2 The sun spectral irradiance measured at the goldsea lake field on 24th September 1989.

DS-1260 was improved into DS-1268 by Daedalus Corp. in 1989. This instrument has fairly good response properties. For requirement of calculation, the relative response function $S_{ri}(\lambda)$ of DS-1268 is normalized to make the response function vs. the same wavelength file (0.4 - 2.5 μm), in Fig.3.

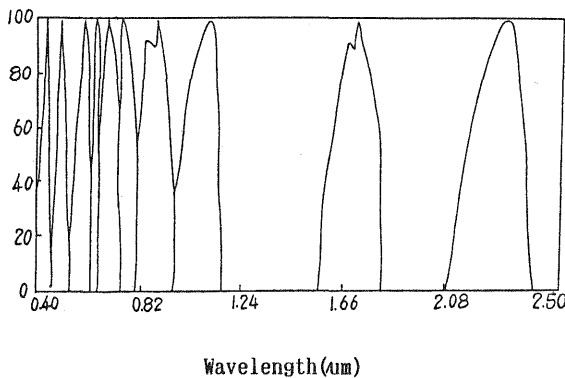


Fig.3 The response function curves of DS-1268 sensor.

3.3 The Synchronization Measurement Technique

The so-called synchronization measurement means that the ground measurements and flight scanning are done at the same time. In the field, it isn't only very difficult that the reflectance is measured full synchronization with the flight scanning, but also impossible. On the basis of theoretical analysis, it is known that the reflective properties have no change in short time; it isn't necessary to measure reflectance of earth objects at the synchronization. While the airplane is overhead in flight scanning, the spectral measurement of the ground only measures the sun radiant energy at this time, then the sun reflective brightness $E_e(\lambda)/\pi$ on the Lambert surface ($\rho = 1$) is obtained. Therefore, make the synchronization measurement be feasible. The cloth targets are placed the nadir of flight line. The same color cloth targets is placed in the scanning line (in Fig. 4) with the equality interval.

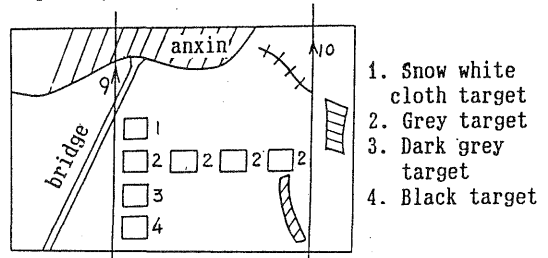


Fig.4 The location of cloth targets placed in anxin field in Hebei province.

3.4 Acquisition Data

The measurements of the ground spectral and airborne multispectral scanning are in the three test fields respectively. The reflectance data of different, ATM data, the sun reflective brightness data (on the standard plate) are acquired. The case of field synchronization measurements is in Table 1.

Test fields	date		height (km)	IFOV (mrad)	scalar of jobs	
	measuring	syncing			curves	objects
goldsea lake	89.9.19 to 9.26	9.24	1	2.5	72	11
gaoyang county	89.12.24 to 12.29	12.24	1	2.5	43	9
anxin county	90.4.24 to 5.9	5.6(2km) to 5.7(2km)	1 & 2	2.5 1.25	76	12

note: The flight of goldsea lake, gaoyang and anxin county is respectively DS-1268 test, detecting oil pipe and investigating pollution.

Table 1. The simple introduction of synchronization measurements in the three test fields.

4. THE METHOD OF PROCESSING DATA

4.1 The Ground and Airborne Data Processing

The reflectances $\rho(\lambda)$ of the different earth objects in the three test fields is

computed. They are the average with a few measurements.

Using relative response function $S_{ni}(\lambda)$ acted as filter functions, according to equation(14), the result of $\rho_j(\lambda)$ multiplied $E_e(\lambda)/\rho_n$ is being integrated, to acquire the efficient reflective brightness L_{ij} of the earth objects in each band (Table 2).

The HDDT (High Density Digital Tape) is transformed into CCT, one finds out the read numbers D_{ij} of natural earth objects and cloth targets. As to cloth targets, the D_{ij} of pixel is read, and the average \bar{D} of pixels selected with natural earth objects is calculated.

iv. The forecast of believability region.

It's known that the reliability region of L_{ij} is between the parallel regression lines (up and down) concerning the enough many samples. If the reliability is 95 percent, the region of L is $\pm 2\sigma$. If it's 99 percent, that is $\pm 3\sigma$. However, the amount of samples isn't very large in the test, the forecast region of L_{ij} is

$$(\hat{a} + \hat{b} * D_{ij}) \pm t^{\alpha/2} (n-2) * \hat{\sigma} * (1 + \frac{1}{n} + (D_{ij} - \bar{D}_{ij})^2 / \sum_{j=1}^n (D_{ij} - \bar{D}_{ij})^2)^{1/2} \quad (22)$$

5. ANALYSIS OF RESULTS AND DISCUSSION

objects	Band										
	D _{ij} /L _{ij}	1	2	3	4	5	6	7	8	9	10
wheat		9.4/0.31	20/0.8	44/1.99	32/0.59	33/1.09	119/4.7	210/12	85/6.01	27/2.70	12/0.94
white cloth target		107/7.2	255/18	255/30	255/10	255/20	255/19	214/33	148/17	100/9.8	55/3.65
grey cloth target		50/3.33	121/8.1	203/13	176/4.6	187/8.9	177/8.3	206/15	84/7.53	71/6.95	48/3.16
dark grey cloth target		15/0.73	33/1.86	61/3.32	51/1.11	61/2.6	92/4.62	211/19	121/13	91/9.64	52/3.6
black cloth target		11/0.23	19/0.56	30/0.90	26/0.32	27/0.65	30/0.65	44/1.30	28/0.79	47/3.53	45/2.32
water		10/0.22	23/0.64	43/1.31	35/0.45	32/0.79	30/0.51	31/0.67	14/0.27	6/0.27	5.5/0.16

Table 2. The data D_{ij} and L_{ij} of Anxin county test field

4.2 Create Relationship

According to the equation(17), by taking the ground and ATM data, the statistic regression equation is created using method of a least squares, and counts the regression and relation coefficients[8]. The regression line is as seen in Fig. 5.

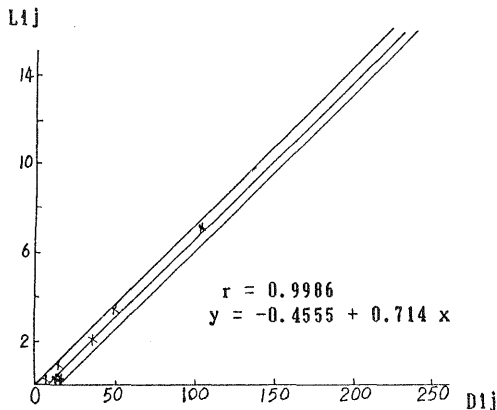


Fig.5 The chart of linear regression between the ground spectral and ATM data of band 1 in flight line nine.

4.3 The Way of Error Estimation and Remarkability Examination[8],[9].

i. The standard deviation estimation of L_{ij}

$$\hat{\sigma} = \left(\sum_{j=1}^n (L_{ij} - \bar{L}_{ij})^2 / (n-2) \right)^{1/2} \quad (20)$$

ii. Standard deviation estimation of b_i :

$$\hat{\sigma}_b = \hat{\sigma} / \left(\sum_{j=1}^n (D_{ij} - \bar{D}_{ij})^2 \right)^{1/2} \quad (21)$$

iii. Gama and T examination[9].

5.1 The Relationship of ATM and The Ground Spectral Data

In the three test fields, the relation coefficients between the six multispectral images and the ground efficient reflective brightness data are as shown in Table 3.

band	test fields γ_i										
	1	2	3	4	5	6	7	8	9	10	
Goldsea lake		.991	.991	.993	.991	.950	.939	.993	.995	.995	
Gaoyang county		.989	.995	.945	.994	.997	.993	.993	.994	.968	.955
Anxin county	9 line	.999	.998	.992	.988	.989	.986	.986	.980	.980	.944
	10 line	.999	.999	.999	.991	.999	.985	.934	.955	.998	.998
	9'' line	.993	.997	.991	.988	.989	.985	.985	.964	.977	.942
	10'' line	.994	.999	.996	.986	.989	.975	.984	.967	.987	.973

Table 3. The fifty nine relation coefficients in the three test fields.

The distribution of relation coefficients in Table 3. is in Figure 6.

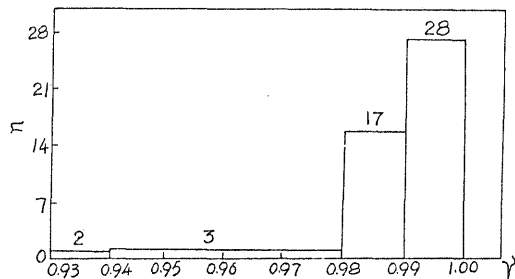


Fig.6 The histogram of the relation coefficients distribution.

One can see the relation coefficient that is greater

than 0.99 have 28 with forty seven percent; the coefficients that are greater than 0.95 have total 54 with 92 percent; the coefficients that are greater than 0.93 have total 59 with 100 percent. When is 0.05 level, in the terms of examination, Gama(0.05) is shown in Table 4.

n	5	6	7	8	9	10
0.05	0.878	0.811	0.754	0.707	0.666	0.632

Table 4. The looking up table of γ (Gama) examination.

The arbitrary in Table 3 is all greater than the maximum(0.878) in Table 4, thus the relationship is fairly remarkable using Gama examination.

In the Table 5, the values of T e.g.,

$$T = |\hat{b}| / \hat{\sigma} * (\sum_{j=1}^n (D_{ij} - \bar{D}_{ij})^2)^{1/2} \quad (23)$$

and $T(e.g., t_{0.025}(n-2))$ are given. The few T is a few times greater than T_0 . The relationship is also very reliability using T examination. The results as above make clear powerful that the relative analysis model created on the airborne and ground data is extremely identical with practical situation.

Fields	band T/T ₀	1	2	3	4	5	6	7	8	9	10
		Goldsea lake		74.4/2.6	14.8/2.8	16.9/2.8	14.6/2.8	6.08/2.8	5.5/2.77	16.5/2.8	23.2/2.6
Gaoyang county		15.1/2.6	22.7/2.6	5.79/2.8	20.2/2.6	27.1/2.8	18.3/2.8	15.3/2.8	20.5/2.6	7.68/2.6	7.16/2.6
Anxin county	9 line	42.4/2.6	31.2/2.6	15.3/2.0	13.0/2.8	13.2/2.8	11.8/2.8	10.2/3.2	11.1/2.6	11.1/2.6	6.40/2.6
	10 line	57.6/2.6	52.5/2.6	41.8/2.8	14.6/2.8	44.9/2.8	11.4/2.0	5.22/2.8	7.16/2.6	32.7/2.6	31.3/2.6
	9'' line	19.2/2.6	23.6/3.2	14.9/2.8	12.6/2.8	13.3/2.8	11.4/2.8	12.6/2.6	8.07/2.6	10.2/2.6	6.28/2.6
	10'' line	20.2/2.6	51.9/2.8	21.2/2.8	11.6/2.8	13.6/2.8	8.75/2.8	12.5/2.6	8.53/2.6	13.5/2.6	9.44/2.6

Table 5. The calculation results of T examination

5.2 Error Analysis

i. Error δb of \hat{b} . The relative error δb is

$$\delta b = (\hat{\sigma} / \hat{b}) * 100\% \quad (24)$$

Fields	band δb	1	2	3	4	5	6	7	8	9	10
		Goldsea lake		1.3	6.7	6.1	6.8	16.4	18.2	6.1	4.2
Gaoyang county		6.5	4.3	17.3	4.8	3.8	5.5	6.6	4.9	12.6	13.0
Anxin county	9 line	2.3	3.2	6.6	7.7	7.5	8.5	9.9	9.0	9.0	15.7
	10 line	1.7	1.9	2.4	6.8	2.2	8.7	19.2	13.9	3.0	3.27
	9'' line	5.2	4.2	6.7	7.8	7.6	8.8	8.0	12.4	9.8	16.0
	10'' line	5.1	1.8	4.8	8.7	7.4	11.8	8.0	11.8	7.3	10.3

Table 6. The relative error δb of each band.

From Table 6, one can see: $\delta b \leq 5$, total 17, occupying 29 percent; $\delta b \leq 10$, total 46, occupying 78 percent; $10 < \delta b \leq 20$, total 13, occupying 22 percent; $\delta b > 20$, total zero. For the almost part error of δb is less than

ten percent, the error δb with few bands is greater than 10 percent, and less than 20 percent. About the band, error δb of the second band is all less than five percent, but the error δb of the seventh and tenth band is greater than the others.

ii. The Error δL of L_{ij} :

The error of L_{ij} is shown clear is drawn using believable region with α (alpha) level (in Fig. 5). In order to simple estimate the error of L_{ij} , δL is defined

$$\delta L = \hat{\sigma} / L_{max} \quad (25)$$

where L_{max} is L_{ij} with the maximum D_{ij} ($D_{ij}=255$). δL expresses the relative errors of L_{ij} to some extent.

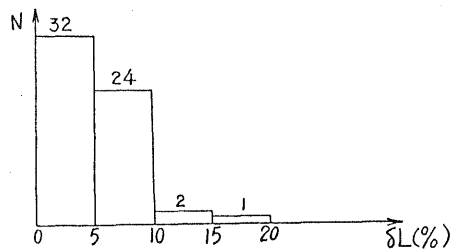


Fig.7 The histogram of δL distribution.

One can see few L is greater than ten in Fig.7. This is because that there is error in the field measurements. The major factors show as:

i. The natural earth objects are not pure, but the Field of View(FOV) of IRIS Spectrometer is small. In the small area measurements, though many times measurements are done, it is difficult to imitate the properties of the large area, and the airborne D_{ij} values are just acquired on the large area(2.5 x 2.5 M²).

ii. The number of typical earth objects is limited. Because the DS-1268 gain level selected is big, the read numbers of some earth objects are saturation, as result, there is no meaning about them. Then the number of earth objects taken part in statistic is less.

iii. The Lambert properties of typical earth objects isn't fairly ideal.

5.3 The Different Flight Heights Affect The Regression Coefficients

Such as the 9 flight line (height is 1 km) and 9'' line(it's 2 km)of Anxin test field in Hebei province. Their IFOV (Instantaneous Field Of View) are 2.5 and 1.25 mrad(it's unit of angle) respectively,and their gain level of each band is the same.

band item data		band									
		1	2	3	4	5	6	7	8	9	10
b	9 line	.071	.073	.064	.025	.045	.047	.072	.123	.103	.062
	9'' line	.030	.029	.059	.022	.040	.042	.161	.095	.038	.019
g	9 line	1	1	1	1	1	1	1	1	1	1
	9'' line	8	8	4	4	4	4	2	8	8	8
g''·b''		3.44	3.12	3.66	3.56	3.50	3.57	4.47	6.17	2.94	2.43
g·b											

Table 7. The data of b,gain,g''b''/gb of the 9 and 9''line in Anxin test field.

From the equation(19),one gets

$$\frac{g_i' \cdot b_i'}{g_i b_i} = \frac{Sp_i \tau_i}{Sp_i' \tau_i'} \quad (26)$$

according to above equation,from Table 7(bottom line, one can see that $Sp_i \tau_i$ is a few times greater than $Sp_i' \tau_i'$.The (1 km)is certainly greater than τ_i' (2 km), and Sp_i of 2.5 mrad is usually greater than Sp_i' of 1.25 mrad. Thus, that the $Sp_i \tau_i$ is greater than $Sp_i' \tau_i'$ is completely identical with practical situation .

Where,one points out,in the test scheme,without making radiance and atmospheric corrections about ATM data, the regression equations are direct created by using the field synchronization measurements technique and statistic analysis method. But the comprehensive effects of atmosphere and sensor is given in the relation coefficients(a_i and b_i).Thus the comprehensive influences of atmosphere and sensor are evaluated with the analysis results, and the influence of atmosphere and sensor are not discussed respectively.

5.4 The Different Detection Angles Affect The Regression Coefficients

In the same multispectral image, the detection angle of the edge is different from that of nadir,and both of their path through atmosphere from earth objects to sensor is different respectively. Thus the atmospheric influence of the edge and center in the same image is different.The test program of different detection angle is arranged along the direction of scanning line.

In the Anxin county test field,the flight heights of 9'' and 10'' lines are all two kilometers, IFOV is 1.25 mrad, the half angle of FOV (Field of View) is 21.48 degree. The different color cloth targets are in the nadir of 9'' flight line, the detection angle of them is about 4.32 degree. The detection angle of them in the flight line 10'' is about 11.82 degree . The difference of detection angle is 7.56 degree.

band item data		band									
		1	2	3	4	5	6	7	8	9	10
\hat{b}	9" line	0.03	0.028	0.059	0.022	0.041	0.042	0.161	0.095	0.038	0.019
	10" line	0.031	0.029	0.056	0.022	0.04	0.039	0.159	0.085	0.036	0.018
\hat{a}	9" line	-1.13	-1.76	-2.55	-0.64	-1.19	-1.87	-4.96	-6.63	-1.27	-0.47
	10" line	-1.27	-1.89	-2.37	-0.65	-1.22	-1.60	-4.20	-5.60	-1.19	-0.50

Table 8. The coefficients \hat{a} and \hat{b} in the 9'' and 10'' flight line.

One can see the difference of the \hat{a} in 9'' and 10'' flight line is negligible. So is the \hat{b} . This is because that the difference of detection angle in two lines is only seven point five six degree. On the satellite image, because the total FOV is 10 degree, the half FOV is about five to six degree. In this case,the different detection angles exert influences in the same image can be neglected.

band item data		band									
		1	2	3	4	5	6	7	8	9	10
\hat{b}	9 line	.0714	.073	.0639	.0245	.0451	.047	.072	.123	.1029	.0619
	10 line	.0867	.0807	.0845	.0353	.0599	.0611	.0887	.1457	.1023	.0683
\hat{a}	9 line	-0.46	-0.9	-0.92	-0.25	-0.41	-0.57	-1.68	-2.66	-0.61	-0.03
	10 line	-0.76	-0.95	-2.26	-0.76	-1.23	-1.68	-2.85	-3.38	-0.32	-0.11
$\frac{\hat{b}_{10}}{\hat{b}_9} = \frac{\tau_9}{\tau_{10}}$		1.21	1.11	1.32	1.44	1.33	1.30	1.23	1.18	0.99	1.10

Table 9. The data of the \hat{a} , \hat{b} and \hat{b}_{10}/\hat{b}_9 in 9 and 10 flight line.Here shows the atmospheric transmittance in 9 line.The \hat{b} shows the evaluation of regression coefficient in 9 line.

From the Table 9, the arbitrary \hat{b}_{10} is all greater than \hat{b}_9 (except 9 band).From the equation(19),one can get transmittance(τ_9)is greater than τ_{10} (gain and Sp_i are not change respectively). The 9 and 10 line flight heights are all one kilometer, IFOV is 2.5 mrad,the half FOV is 42.96 degree. The cloth targets (different color) is in the nadir if 9 line, its detection angle is 11.1 degree. The cloth targets is viewed in 10 line, its detection angle is 42.24 degree. The atmospheric path from targets to sensor in the ten line is longer than that of nine flight line, its influence of ten line is certainly bigger than that of nine line, its transmittance in 10 line is less than one of 9 flight line.Therefore the its influence at the image edge is greater than that of image center, in the same image with the detection angle variation being quite big, the brightness of image at the edge is darkened clearly.

5.5 Generate the Efficient Reflective Brightness Image of the Ground

In the terms of the regression equation ($L = a + bD$), the multispectral data (DN) are transformed into the efficient reflective brightness image of ground. In this way, airborne multispectral image of reflective brightness is gotten, it isn't an original image.

Because the digital number of efficient reflective brightness is very small, the image splendour of direct display is very dark, a suitable transformation on number is made, or, give a fit brightness to image. Let

$$L' = \frac{255}{L_{max}} L = P * L \quad (27)$$

then

$$L' = P(b * D + a) = P * b(D + \frac{a}{b}) = P * b(D - D_s)$$

that is

$$L' = P * b(D - D_s) \quad (28)$$

where L' is the grey-level of efficient reflective brightness image. L_{max} is the brightness v.s. D_{max} (255). D_s is the read number of DS-1268 without the reflection of earth objects. It includes the atmospheric radiance and the zero response (no energy entering) values of sensor.

Although, the equation (28) is the linear transformation of image, there is particular meaning about it. The result of it is an image of the efficient reflective brightness of ground, so that the image is used in the quantitative application and analysis.

For instance, processing the third band of 9'' flight line in the Anxin test field, the regression equation is

$$\begin{aligned} L &= 0.0585 * D - 2.551 \\ &= 0.0585 * (D - 43.6) \end{aligned} \quad (29)$$

then the splendour P of image is

$$255 / 12.4 \quad (W/M^2 \cdot Sr)$$

Thus,

$$L' = \frac{255}{12.4} L = 1.2 * (D - 44) \quad (30)$$

As about the equation (30), the image of original digital number D is transformed into the image of efficient reflective brightness of the ground (in Fig.8). The right half part in Fig.8 is the image of original data D , the left half part is the image of efficient reflective brightness of the ground. By comparison with the images of right and left part, the image of 9''B3 signed covers a coat "white fog" clearly (as a result of the atmosphere radiance and sensor zero response), but the atmospheric effects and sensor's zero response in the image signed 9''R3 of efficient reflective brightness is removed. Thus, the contrast of later (9''R3) is very apparent, its levels are getting increase. Their histogram is shown in Fig.9 and Fig.10 respectively.

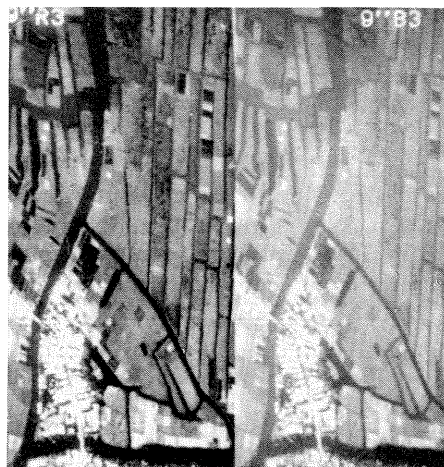


Fig.8 The image of the original and efficient reflective brightness.

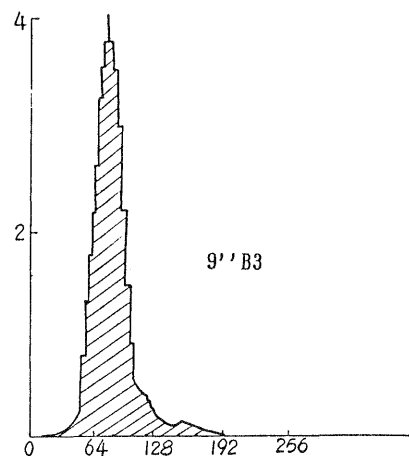


Fig.9 The histogram of original image in the third band.

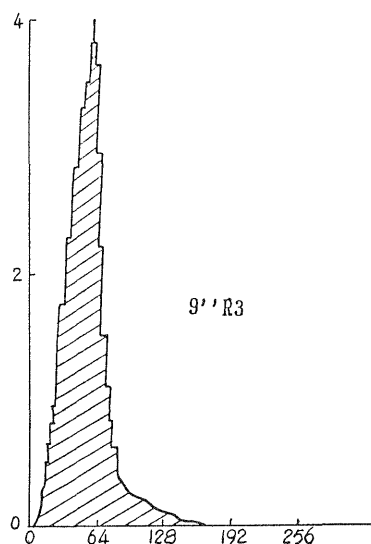


Fig.10 The histogram of efficient reflective brightness of the ground in the third band.

6. CONCLUSION

The more deep analyses have been done from theory about the relation of ATM and the ground spectral data in this paper, the linear relation between the ATM data and efficient reflective brightness of the ground is determined, and the definite physical meaning on the relation coefficients is given.

During flight test of the Gold-sea lake, Gao yang county and Anxin county, the synchronization measurements of the reflectance spectral of the earth objects were carried out from the fall in 1989 to the summer in 1990, and the solar irradiance spectra on the ground was obtained at the same time. On the base of a great of measurements, according to the theoretic model, using the statistical regression analysis the linear regression equations from different bands, flight lines and test fields were gotten. By the Gama and T examination about the relationship, the results of examinations show the relationship is fairly remarkable. Thus, it supports powerfully the mathematical model created in the theory analysis.

The influence of the regression coefficients with the different flight heights and detection angles is approached. The result shows, because of different gains of the sensor (with different sensitivity) and the atmospheric influence in the different flight heights test of one km and two km, that they make the regression coefficients have great difference. If the variation of detection angle is not big (e.g., 5 to 7 degree, for instance the image of satellite), the influence caused by the change of detection angle may be ignored. But, the detection angle has great change from center to edge in the ATM image (it's greater than forty degree), the influence of that is very obvious. Its more detail regular pattern need be still studied further.

According to the linear regression equation gotten by the test, the airborne original digital image is transformed into the image of efficient reflective brightness of the ground. The comprehensive influences caused by atmosphere and sensor are eliminated. It corresponds to dealing with the radiant and atmospheric corrections. It establishes a foundation for the farther quantitative analysis research.

7. REFERENCE

- [1] Fong J.J., Yu B.X., 1981. The colourscope methodology of the multispectral remote sensing image proceeding. The Collection of Papers On Chang Chun Remote Sensing Test.
- [2] Gou d. f., 1985. The computer proceeding and pattern recognition of remote sensing image. Published by the Electric Industry publishing.
- [3] 1983. Definition of atmospheric radiance and transmittances in remote sensing. Remote Sensing of Environment. Vol. 13, pp. 89-92.
- [4] Philip H. S., Shirley M. Davis. 1978. The Quantitative Approach of Remote Sensing. pp. 1-73.
- [5] Tong Q.X. et al, 1980 - 1990. The acquisition, processing and analysis of Ku Che region in XinJiang province about the airborne remote sensing data. The Practice and Achievement of Application of for Remote Sensing.

[6] Zhuang P. R., Zhao B. Y. 1986. The Reflective Spectral Theory, Methodology and Geological Application of The Earth Objects. The Remote Sensing And Geological Application Research. pp. 2-41.

[7] The Atmospheric Influences On Remote Sensing Measurements. <E -- 26818 --U> Vol. 1, The Abstract of Report.

[8] Zhe Jiang University Math. Dept., 1980s. Probability and Mathematical Statistics. Published by People's Publishing House.

[9] Zhou X.Z., Zhou D.C., 1980s. Probability and Mathematical Statistics. Published by People's Publishing House in He Long Jiang Province.